JAST. Vol. 9, No. 1, pp 59-73

JAST
Journal of Aerospace Science and Technology

Crack Analysis, Using a New Coupled FE-EFG Method

S. Mohamadnejad[1], A. Darvizeh[2], M. Darvizeh[2], R. Ansari[3], and A. Basti[4]

To solve crack problems, some coupled methods have been developed in recent years. Most of these methods have some shortcomings such as the need for a transition region. The finite element and enriched element free Galerkin methods are widely used for this class of problems. In order to take the advantages of these methods while avoiding the disadvantages, it is essential to follow solution approaches based on a combination of them. Prompted by this idea, in this article, the authors mainly aim at finding a simple way to solve the problem of a cracked plate by using a novel coupled finite element-element free Galerkin (FE-EFG) method. In this procedure, the usage of transition region is bypassed by employing the concept of "virtual particles". The enriched element free Galerkin method is applied to approximate regions near a crack tip and the finite element method is put to use in the areas far from the crack tip. Static analysis of two-dimensional crack problems, according to the plane stress condition under mode-I loading, has been done. The results from the present method are indicated to be in excellent agreement with those from the existing analytical solutions.

1 Introduction

The finite element method (FEM) [1, 2] has been recognized as an appropriate simulation procedure for a large number of problems in various branches of engineering and science. This wide usage has delineated its defects and benefits. Some problems are unsolvable or are hard to solve by the FEM; for example, problems which deal with crack growth and those with intricate configuration can be noted. Therefore, researchers endeavor to find new solution techniques or to improve the FEM. Among these alternative methods, one can mention meshfree or meshless methods [3]. The first meshfree method proposed by Lucy [6] is smooth particle hydrodynamic (SPH) [4, 5]. After that, several other meshfree methods were developed (e.g. the diffuse elements (DEM) by Nayroles et al. [7], the element free Galerkin (EFG) method by Belytchsko et al. [8-10], the reproducing kernel particle method (RKPM) by Liu et al. [11] and the meshless local Petrov-Galerkin (MLPG) method by Atluri and Zhu [12, 13]). Meshfree methods are suitable for solving hard differential equations in engineering and in other scientific areas. It has been revealed that, in some aspects, they are superior to their conventional counterparts such as the FEM, the boundary element method (BEM) and the finite difference method (FDM). For instance, some engineering problems which involve very large distortion, dynamic fracture, cracks or explosion cannot be solved by the classical methods, whereas the meshfree approaches are found to be capable of solving them. However, meshfree methods have some defects such as considerable computational cost, difficult imposition of essential boundary conditions and complexity in the analysis of problems with point loads.

Considering the limitations and advantages of meshfree methods and those of the FEM, finding procedures for combining these methods seems to be useful. One reason that necessitates the need for combining the FEM with meshless methods is associated with the fact that imposing boundary conditions sometimes becomes very difficult. There are many works in the literature in which coupled meshless-finite element methods (e.g. EFG-FEM, MLPG-BEM and MLPG-FEM) have been developed. Using "virtual elements", Hegen [14] offered an approach for combining meshless methods based on the moving least square (MLS) method and the FEM. The EFG-FE method suggested by Belyschko[15] is the most prominent coupled method.

As it is well-known, in meshless methods, instead of a structured mesh, only a dispersed set of nodal points is needed. This feature can be helpful for modeling crack

1. M.Sc., Graduate Dep't of Mech. Eng., Univ. of Guilan, Guilan, Iran.

2. Professor, Dep't. of Mech. Eng., Univ. of Guilan, Guilan, Iran.

3. Assistant Professor, Dep't. of Mech. Eng., Univ. of Guilan, Guilan, Iran, E-mail:r_ansari@guilan.ac.ir.

4. Assistant Professor, Dep't. of Mech. Eng., Univ. of Guilan, Guilan, Iran.

propagation. In addition, although meshless methods are adaptable for modeling crack propagation, they are more time-consuming than the FEM because of their changeability. Therefore, it is essential to use meshless methods in the area of crack growth and the FEM in other areas of the domain. Many researchers have already used different coupled methods to analyze crack problems. For example, Rao and Rahman [16] have used interaction integral to couple the EFG with the FEM. Gu and Zhang [17] have used transition region (or bridge region) that can be discretized by transition particles. Xiao and Dhanasekar [18] have utilized a collocation approach to couple FEM with EFG.

In this paper, based on the EFG-FEM coupling method suggested by Hsun and Ping [19], an enriched EFG-FEM coupling method is proposed for the crack problem.

Four techniques are used to simulate discontinuities in the meshfree method: (i) improvement of the weight function similar to the visibility, diffraction and transparency methods [20, 21], (ii) improvement of the intrinsic basis [22], (iii) methods established on an extrinsic MLS enrichment [22], and (iv) methods established on the extrinsic PUM enrichment [23]. The increased Lagrangian method has been employed to simulate powerful discontinuity (crack problems) in Carpinteri [24] and powerless discontinuity in Carpinteri [25].

2 An Overview on Element Free Galerkin Method

The EFG method suggested by Belyschko et al. [26] is based on the diffuse element method (DEM)[27]. Some of the important characteristics of the EFG method are as follows:

1. In this method, moving least square (MLS) technique is employed for shape function construction,
2. The Galerkin weak form method is used to discretize the system of equations, and
3. Cells of mesh are necessary for computations of integration related to the matrix of system.

The equilibrium equation in the EFG method for a body that occupies the domain Ω with the boundary of Γ is written as follows:

$$\nabla.\sigma + b = 0 \qquad \dot{n} \quad \Omega\,, \tag{1}$$

where, σ is th ınress tensor, which fits into the displacement field u, ь ıs the body force and ∇ is the divergence operator. The boundary conditions are:

$$n.\sigma = \bar{t} \text{ ı on } \Gamma_t \quad u = \bar{u} \quad \text{on } \Gamma_u \tag{2}$$

Both FE and EFG methods use a weak form of Equations 1 and 2. To apply the variational method, we employ the total potential energy as:

$$\Pi = \frac{1}{2}\int_{\Omega} \varepsilon^T D\varepsilon d\Omega - \int_{\Omega} u^T .\mathrm{bd}\,\Omega - \int_{\Gamma_t} u^T .\bar{t} d\Gamma_t \tag{3}$$

where, D denotes the matrix of material properties, *u* is the displacement field, *n* is the perpendicular unit vector, *b* is the body force, $\bar{u}$ is the imposed displacement at boundary Γ and $\bar{t}$ is the imposed stress.

To approximate the displacement field, the following polynomial functions with variable coefficients are used:

$$\begin{aligned} u^h(x) &= \sum_{i=1}^{m} p_i(x) a_i(x) \\ &= p^T(x) a(x) \end{aligned} \tag{4}$$

in which, $p_i(x)\ i = 1,2,\ldots,m,$ are monomial basis functions, *m* is the number of terms in the basis, and $a_i(x)$ are the coefficients of the basis functions.

Overview on Moving Least Square Method

The moving least square (MLS) method was recommended by Lancaster and Salkauska [28] to approximate the shape function of the EFG. MLS approximation has two main properties: First, the approximation of field function is continuous and smooth. Second, it can present an approximation with the requested order of consistency. The approximation of field function in MLS is done via Eq. 4. The basis functions are given by:

$$\text{in two–dimensional } p^T = (1, x_1, x_2)\,. \tag{5}$$

The interpolation at x can be expressed as follows [28]:

$$\begin{aligned} u^h(x, x_i) &= \sum_{i=1}^{m} p_i(x_i) a_i(x) \\ &= p^T(x_i) a(x) \end{aligned} \tag{6}$$

where, x_i is the point in the MLS-interpolation of x. To obtain the interpolation of the function *u(x)*, the difference of the interpolation $u^h(x)$ and the function u(x) must be minimized by a weighted least squares method. For the functional, we have:

$$J = \sum_{I=1}^{n} w(x-x_I)[u^h(x,x_I)-u(x_I)]^2 = \sum_{I=1}^{n} w(x-x_I)\left[\sum_{i=1}^{m} p_i(x_i)a_i(x)-u(x_I)\right]^2, \quad (7)$$

where, $w(x-x_I)$ is the weight function and $x_I\,(I=1,2,...,n)$ are nodes covering the point x. We can rewrite Equation (7) as:

$$J = (Pa-u)^T W(x)(Pa-u), \quad (8)$$

where,

$$u^T = (u_1, u_2, \ldots u_n) \quad (9)$$

$$P = \begin{bmatrix} p_1(x_1) & p_2(x_1) & \cdots & p_m(x_1) \\ p_1(x_2) & p_2(x_2) & \ldots & p_m(x_2) \\ \vdots & \vdots & \ddots & \vdots \\ p_1(x_n) & p_2(x_n) & \ldots & p_m(x_n) \end{bmatrix}, \quad (10)$$

$$W(x) = \begin{bmatrix} w(x-x_1) & 0 & \ldots & 0 \\ 0 & w(x-x_2) & \ldots & 0 \\ \vdots & \vdots & \ddots & \vdots \\ 0 & 0 & \ldots & w(x-x_n) \end{bmatrix}, \quad (11)$$

Then, from:

$$\frac{\partial J}{\partial a} = 0, \quad (12)$$

we have:

$$A(x)a(x) = B(x)u \quad (13)$$

where, A is nominated weighted moment matrix which can be given by:

$$A(x) = P^T W(x) P\ , \quad (14)$$
$$B(x) = P^T W(x)\ .$$

From Eq. 13, we have:

$$a(x) = A^{-1}(x)B(x)u. \quad (15)$$

The local approximation $u^h(x)$ is thus:

$$u^h(x) = \Phi(x)u = \sum_{I=1}^{n} \Phi_I(x)u_I\ , \quad (16)$$

where, $\Phi(x)$ is the shape function with the following formula:

$$\Phi(x) = (\Phi_I(x)\ \Phi_2(x)\ \ldots, \Phi_n(x), = P^T(x)A^{-1}(x)B(x). \quad (17)$$

It should be noted that, in this study, linear polynomials are used.

3 Weight Function

The selection of weight function in the MLS method is very substantial. In this regard, consider the following points:

- weight function is explained as the function of the distance between two points [29],
- support must be fitted into a small space, i.e. outside the support domain is zero, and
- all points in the support domain must have positive values.

Different weight functions have been used in various references.

We approximate the displacement field in the following form:

$$u^h(X) = \{p(X)\}^T [[P][W][P]^T]^{-1}[[P][W]]\{u\}, = \Phi(X)\{u\} \quad (18)$$

The shape function of each particle can be obtained as

$$\Phi(X) = \{p(X)\}^T [[P][W][P]^T]^{-1}[P][W]]\cdot \quad (19)$$

4 Enriched EFG

The goals of the enriched EFG are

- finding non-enriched and enriched particles,
- handling extra degrees of freedom,
- calculation of stiffness matrices.

The choice of supplemented particles is clarified in Fig. 1. It is adequate to calculate the marked space from the particles to the crack and the space from the particles to the crack front and linked these spaces with the radius of the support area. Because of the existence of extra degrees of freedom (DOF's), the assembly process has to be revised. Some imaginary nodes were applied to manage these extra dofs. These nodes are named "Phantom nodes". At H-enriched node and at a front enriched node, one phantom node and four phantom nodes were added, respectively. Addition of these imaginary nodes begins from the complete number of exact nodes plus one.

In two-dimensional problems, at a particular node assigned by a number i, there are two unknowns that are associated with equation numbers 2i − 1 and 2i in the global matrix. If it is a discontinuous-enriched node, it contains two supplemental unknowns that are associated with equation numbers 2 × pos(i) − 1 and 2 × pos(i) in the global matrix. Therefore, if it is an adjacent front enriched node, it contains eight supplemental unknowns from equation numbers (2×pos(i)−1, 2× pos(i)), (2 × (pos(i) +1) − 1, 2 × (pos(i) + 1)), (2 × (pos(i) + 2) − 1, 2 × (pos(i) + 2)) and (2 × (pos(i) + 3) − 1, 2× (pos(i) + 3)), where every couple matches every supplemented phantom node.

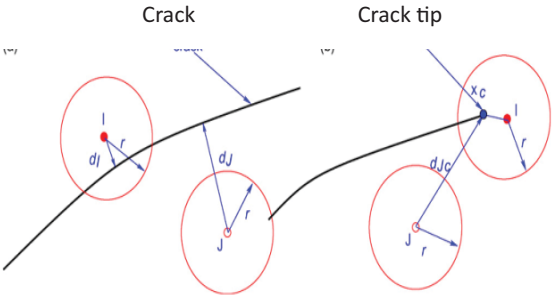

Figure 1. Assortment of enriched particles: (a) Discontinuous enriched particles, (b) Close to front enriched particles [3].

The ordinary section and the enriched section are components of the B matrix at a Gauss point gp. The ordinary section is constantly calculated but the enriched section is just calculated if, in the nodes whose supports comprise gp, there are enriched nodes [3].

In equation (20), B^{std} is the standard B matrix and B^{enr} is the enriched B matrix: where ΦI(x) can be either the Heaviside function H(x), or the branch functions Bα(x). The above-mentioned B matrix can be written in the following form:

$$B_I^{enr} = \begin{bmatrix} (\Phi_I)_{,x} + \Psi_I + \Phi_I(\Psi_I)_{,x} & 0 \\ 0 & (\Phi_I)_{,y}\Psi_I + \Phi_I(\Psi_I)_{,y} \\ (\Phi_I)_{,y}\Psi_I + \Phi_I(\Psi_I)_{,y} & (\Phi_I)_{,x}\Psi_I + \Phi_I(\Psi_I)_{,x} \end{bmatrix} \tag{20}$$

$$B_I^{enr} = \begin{bmatrix} B^{Std} & | & B^{enr} \end{bmatrix}$$

5 Numerical Examples:

Infinite Plate Having a Ccnter Crack

We consider an infinite plate that includes a direct crack of length 2a. The plate is subjected to a steady stress field σ. Along ABCD, the closed form solution in polar coordinate (r,θ) is given by

$$u_x(r,\theta) = \frac{2(1+\nu)}{\sqrt{2\pi}}\frac{K_I}{E}\sqrt{r}\cos\frac{\theta}{2}(1-2\nu+\sin^2\frac{\theta}{2}) \tag{20}$$

$$u_y(r,\theta) = \frac{2(1+\nu)}{\sqrt{2\pi}}\frac{K_I}{E}\sqrt{r}\sin\frac{\theta}{2}(2-2\nu-\cos^2\frac{\theta}{2}) \tag{21}$$

$$\sigma_x = \sigma_0\sqrt{\frac{a}{2r}}\cos\frac{\theta}{2}(1-\sin\frac{\theta}{2}\sin\frac{3\theta}{2}) \tag{22}$$

$$\sigma_y = \sigma_0\sqrt{\frac{a}{2r}}\cos\frac{\theta}{2}(1+\sin\frac{\theta}{2}\sin\frac{3\theta}{2}) \tag{23}$$

$$\sigma_{xy} = \sigma_0\sqrt{\frac{a}{2r}}\sin\frac{\theta}{2}\cos\frac{\theta}{2}\cos\frac{3\theta}{2} \tag{24}$$

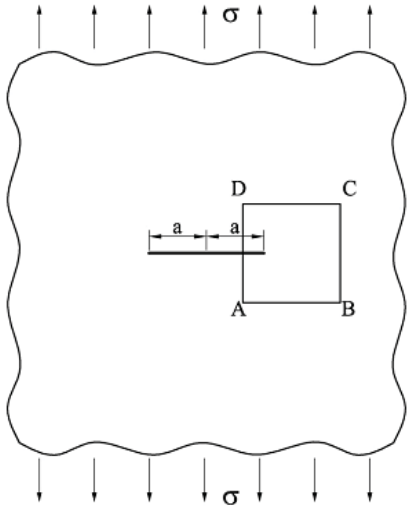

Figure 2. Infinite plate having a center crack subjected to tension [3].

Here, $K_I = \sigma\sqrt{\pi a}$ is the stress intensity factor, υ is Poisson's ratio and E is Young's modulus. ABCD is a square area with the size of 14mm × 14 mm. Also, a = 100 mm, E= 30×10^6 N/mm2, υ=0.3 and σ = 10^4 N/mm2. The geometry of ABCD is shown in Fig. 2. Displacement of nodes on the bottom, right and top edges are obtained from Eq's. (20) and (21).

In other words, boundaries on the bottom, right and top edges are exposed to the known displacements.

The stresses can be obtained from Equations (22-24). The crack is analyzed by the coupled method that will be explained in Section 5. Using 4×4 Gauss Quadrature rule, numerical integration is performed on a background mesh of 13×13 elements. The energy error norm for this combined method is depicted in Fig. 4- a.

KI is the stress intensity factor for mode I contingent upon the crack length, the geometry of example and the implemented loading, and (r,θ) are the polar coordinates of a point after utilizing trigonometric variables. It can be shown that the entire functions which are displayed in Equations (22, 23, 24) are extended across four basis functions which come next:

(25)

$$\left\{ \sqrt{r}\cos\frac{\theta}{2} \;\; \sqrt{r}\sin\frac{\theta}{2} \;\; \sqrt{r}\cos\frac{\theta}{2}\sin\theta \;\; \sqrt{r}\sin\frac{\theta}{2}\sin\theta \right\}$$

In applying the meshless method to linear elastic fracture mechanics (LEFM), it is beneficial to add these four basis functions in Eq. 25 to the linear basis functions, so the stress singularity is able to be entrapped. It was initially applied by Fleming et al. [30] in the element-free Galerkin (EFG) method. Supplementing these four basis functions in Eq. 25 into Eq. 5, the enriched basis functions for two-dimensional problems can be achieved.

a) Complete linear monomials:

$$P^T(x) = [1, x, y, \sqrt{r}\cos\frac{\theta}{2}, \sqrt{r}\sin\frac{\theta}{2}, \sqrt{r}\cos\frac{\theta}{2}\sin\theta, \sqrt{r}\sin\frac{\theta}{2}\sin\theta] \quad (26)$$

b) Complete second-order monomials:

$$P^T(x) = [1, x, y, x^2, y^2, \underset{x\,y}{x}, \sqrt{r}\cos\frac{\theta}{2}, \sqrt{r}\sin\frac{\theta}{2}, \sqrt{r}\cos\frac{\theta}{2}\sin\theta, \sqrt{r}\sin\frac{\theta}{2}\sin\theta] \quad (27)$$

The method that comprises the crack front enrichments yields more precise answers and more superior convergence. With extrinsic MLS enrichment, the most precise answers and the elevated convergence are acquired. Anyway, the calculative price is further costly. Extrinsic MLS enrichment is more precise than the extrinsic PU enrichment.

The identical consideration can be constructed for local convergence. The fact that SIFs can be straightly procured is a great utility of the extrinsic MLS enrichment and this utility apparently results in more precise answers considering local convergence. Figure 4(a) shows the energy error norm for mode I by applying the extrinsic MLS enrichment.

By joining two enrichment functions, cracks are simulated. One for the intricate style at the crack front and a Heaviside step function to execute the discontinuity through the crack. The Heaviside function carries a quantity of 1 over the crack and -1 under the crack inserting a displacement discontinuity through the crack in elements in which the crack disconnects their supports. For the tip of the crack, the enrichment function is used which has been suggested by Fleming to be utilized in the element free Galerkin method.

They were, afterwards, accepted by Belytschko[5] for utilization in XFEM. These functions bridge the crack front displacement area. In addition, observe that the initial function is discontinuous through the crack inside the element including the crack tip.

5 Coupling Technique

For simultaneous utilization of the premium of both EFG and FE Methods, up to now, various combined methods have been submitted. For instance, a convenient collocation approach has been demonstrated by Xiao and co-workers [18]. Also, Gu and Zhang [17] have conducted a lot of research on combining meshless–finite element that uses particles in the transition zone. Ming and Cheng [31] could reach higher precision results by offering a new ramp function to combine element free Galerkin and the finite element method. Combined methods that have been suggested hitherto for combining meshless methods with the FEM can be

categorized in the following way:

- Coupling with ramp functions,
- Coupling with reproducing conditions,
- Handshake (Bridging domain) coupling,
- Strong hybrid coupling,
- Master-slave coupling, and
- Continuous Blending Method (CBM) developed.

The method utilized in this article requires the transition region and its transition region is a line. Virtual particles are placed in the line. Using FEM formulation, the virtual particles have been obtained and utilized as a particle in the element free Galerkin method. In comparison with other coupled methods, this method does not necessitate explanation of the ramp function, Lagrange multipliers, bridging domain or any special processing such as the utilization of visibility criterion in the hybrid approximation.

The conclusive system equation for finding the answer to elastic problems is shown as:

$$[K]\{u\} = \{f\} \tag{28}$$

In this formula, K is stiffness matrix (made of very 2×2 sub-matrices K_{ij}):

$$K_{ij} = \int_{\Omega} B_i^T D B_j + \alpha \int_{\Gamma_{ui}} \Phi_i S \Phi_j \tag{29}$$

$$S = \begin{bmatrix} s_x & 0 \\ 0 & s_y \end{bmatrix} \tag{30}$$

$$s_x = 1 \quad if\ prescribed \quad u_x$$
$$s_y = 1 \quad if\ prescribed \quad u_y$$

where, B_i, B_j are given in Equation (14) and Φ_i, Φ_j are given in Equation (17). To couple the enriched EFG with the FEM, we use B^{er} with some modifications instead of B_i *and* B_j. Also, note that α is a penalty number.

The corresponding load matrix f can be obtained as:

$$f_i = \int_{\Gamma_t} \phi_I \bar{t} d\Gamma_t + \int_{\Omega} \Phi_I b d\Omega + \alpha \int_{\Gamma_{ut}} \overline{\Phi}_i S \overline{u_I} \tag{31}$$

where, $\bar{t}$ is the traction force along the line, b is the body force on a volume and indicates the displacement boundary conditions.

All nodes utilized in the FEM domain possess independent degrees of freedom. The gatherings of stiffness matrix and load vector are alike as can be seen in Eq's. 29 -31.

Normal and virtual particles used in the EFGM domain are obtained from nodes and, hence, possess dependent degrees of freedom. Stiffness values computed for virtual particles are supplemented to matching nodes.

Degrees of freedom in Eq. 29 can be divided into four sections that can be written as follows. The first section is connected to normal particle i and normal particle j.

$$K_{ij} = \int_{\Omega} B_i D B_j d\Omega + \alpha \int_{\Gamma_{ui}} \overline{\Phi}_i S \overline{\Phi}_j d\Gamma_{ui} \tag{32}$$

The second section is connected to virtual particle l and normal particle j.

$$K_{lj} = T_{il}^T \int_{\Omega} B_i^T D B_j d\Omega + T_{il}^T \alpha \int_{\Gamma_{ui}} \overline{\Phi}_i S \overline{\Phi}_j d\Gamma_{ui} \tag{33}$$

The third section is connected to normal particle i and virtual particle n.

$$K_{in} = \int_{\Omega} B_i^T D B_j d\Omega T_{jn} + \alpha \int_{\Gamma_{ui}} \overline{\Phi}_i S \overline{\Phi}_j d\Gamma_{ui} T_{jn} \tag{34}$$

The fourth section is connected to virtual particle l and virtual particle n.

$$K_{ln} = T_{li}^T \int_{\Omega} B_i^T D B_j d\Omega T_{jn} + \alpha T_{li}^T \int_{\Gamma_{ui}} \overline{\Phi}_i S \overline{\Phi}_j d\Gamma T_{jn} \tag{35}$$

where, D is the elasticity matrix, is the standard finite element strain-displacement matrix and $\Phi(x)$ is the shape function given in Eq. 17.

The transformation matrix is as follows:

$$T_{jn}= \begin{bmatrix} N_{i1}(\xi_j,\eta_j) & 0 & \dots N_{i8}(\xi_j,\eta_j) & 0 \\ 0 & N_{i1}(\xi_j,\eta_j) & \dots 0 & N_{i8}(\xi_j,\eta_j) \end{bmatrix} \quad (36)$$

where T_{jn} connects virtual particle j to element n, N_{ni} is the shape function for node i in element n and (ξ_j,η_j) is the coordinate for virtual particle j in element n.

Correspondingly, the calculation of force vector, i.e. Eq. 31, can be extracted as goes next.

The first section is related to normal particle i:

i:

$$f_i = \int_{\Gamma_t} \overline{\Phi}_i \bar{t} d\Gamma + \int_{\Omega} \overline{\Phi}_i b d\Omega + \alpha \int_{\Gamma_{ui}} \overline{\Phi}_i S\bar{u} d\Gamma_{ui} . \quad (37)$$

The second section is connected with virtual particle l as:

$$f_l = T_{il}^T \int_{\Gamma_t} \overline{\Phi}_i t d\Gamma + T_{il}^T \int_{\Omega} \overline{\Phi}_i b d\Omega + T_{il}^T \alpha \int \overline{\Phi}_i S\bar{u}_i d\Gamma_{ui} . \quad (38)$$

6 Determination of the Stress-intensity Factor (SIF)

Utilization of the EFG in crack analysis is very notable and uncomplicated; therefore, it permits simulation of clearly different geometric discontinuities. The stress intensity factor (SIF) in the LEFM is the principal variable capable of characterizing the stress area in the nearby area of the crack front. Its appointment is a critical act. It can be achieved from the stress field, the displacement area or through energy amounts like the famous path-independent integrals as defined by Rice and Rosengre (1968) [33]. In agreement with the J-integral formula, it can be obtained by using the divergence theorem; for instance, one can explain the rate of extricated energy per unit crack propagation in the xk vector [33]:

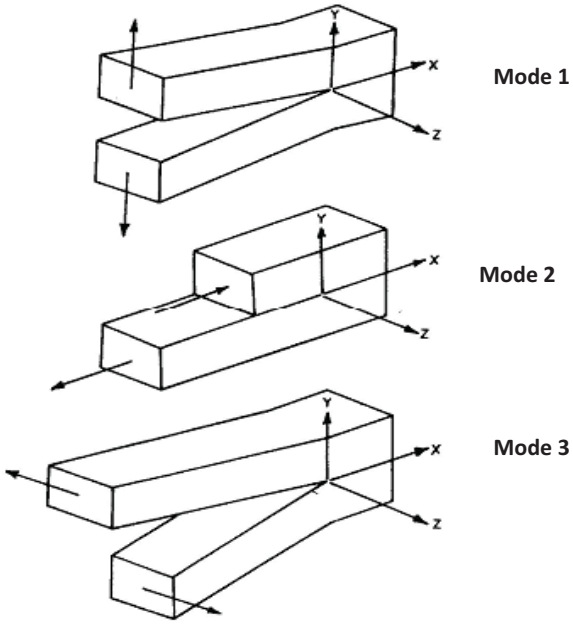

Figure 3. The three modes of failure [34].

$$J_k = \int_{\Lambda} \left(W_{nkk} - t_j u_{j,k} \right) d\Lambda, \quad k = 1,2 . \quad (39)$$

Λ is a general contour enclosing the crack tip (being a part of a surface perpendicular to the crack tip), $W = \frac{1}{2}\sigma.\varepsilon$ is the strain energy density and $t_j = \sigma_j n_i$ are the traction estimated in the direction of the contour Λ, and nj is an outward unit vector perpendicular to contour Λ. The associations among the integrals and the SIFs are the famous [33]:

$$J_2 = 2\frac{K_I K_I}{E'}, \quad (40)$$

in which, $E' = E$ is for plane stress conditions and $E' = E(1-v^2)$ is for plane strain conditions.

The utilization of Eq. 38 for combined mode fracture is restricted due to the hardships in separating mode I and mode II SIFs from the J-integral parts. The segregation of the elastic area into symmetric and anti-symmetric parts [33, 35] leads to an ordinary estimation of the SIFs. Actually, the integral J1, for example, can be mentioned as the supplement of the following two terms:

$$J_1 = J_1^I + J_1^I . \quad (41)$$

The symmetric and anti-symmetric sections of the disintegration can be clearly shown as:

$$J_k^M = \int_\Lambda \left(W^M n_k - t_j^M u_{j,k}^M\right) d\Lambda, \quad k = 1,2; M = I, II \cdot \tag{42}$$

The symbols I and II are assigned to the symmetric and anti-symmetric modes, respectively. We can separate the displacement area into a symmetric and an anti-symmetric part as can be seen in the following matrices:

$$\begin{Bmatrix} u_1 \\ u_2 \end{Bmatrix}_p = \begin{Bmatrix} u_1^I + u_1^I \\ u_2^I + u_2^I \end{Bmatrix}, \quad \begin{Bmatrix} u_1^{'} \\ u_2^{'} \end{Bmatrix}_{p'} = \begin{Bmatrix} u_1^I - u_1^I \\ -u_2^I + u_2^I \end{Bmatrix}, \tag{43}$$

where,

$$\begin{Bmatrix} u_1^I \\ u_2^I \end{Bmatrix}_p = \frac{1}{2}\begin{Bmatrix} u_1 + u_1^{'} \\ u_2^I - u_2^{'} \end{Bmatrix}, \quad \begin{Bmatrix} u_1^I \\ u_2^I \end{Bmatrix}_{Antisymm^{'}} = \frac{1}{2}\begin{Bmatrix} u_1 - u_1^{'} \\ u_2 + u_2^{'} \end{Bmatrix}. \tag{44}$$

The stress area can be divided into a symmetric σ_{ij}^I and an anti-symmetric part σ_{ij}^I which can be achieved as described below:

$$\begin{Bmatrix} \sigma_{11}^I \\ \sigma_2^I \\ \sigma_{12}^I \end{Bmatrix}_{symm} = \frac{1}{2}\begin{Bmatrix} \sigma_1 + \sigma_1^{'} \\ \sigma_2 + \sigma_2^{'} \\ \sigma_{12} - \sigma_{12}^{'} \end{Bmatrix}, \tag{45}$$

$$\begin{Bmatrix} \sigma_{11}^I \\ \sigma_2^I \\ \sigma_{12}^I \end{Bmatrix} A_{symm} = \frac{1}{2}\begin{Bmatrix} \sigma_1 + \sigma_1^{'} \\ \sigma_2 + \sigma_2^{'} \\ \sigma_{12} - \sigma_{12}^{'} \end{Bmatrix}.$$

The concept of the tip is identical with what was mentioned previously about the displacements. J_1^I and J_1^I are calculated as [33]:

$$J_1^I = \frac{k_I^2}{E^{'}} \; J_1^I = \frac{k_I^2}{E^{'}} \cdot \tag{46}$$

Many different methods have been used for crack analysis. Among them, the extended finite element method (XFEM) [36] can be mentioned. Widespread meshfree methods [37-41] are used for crack simulation. The crack discontinuities are corrected by the visibility criterion or certain changes in discontinuities. Other new techniques which can correct twisted and bended cracks were recommended by Ventura et al. [42]. These techniques improved the basis functions of MLS surrounding the crack tip and the convergence manner meaningfully.

The extended element free Galerkin (XEFG) technique was suggested by Rabczuk and co-workers for cohering crack beginning, expansion and connection in two and three-dimensional statics and dynamics; however, the closing of the crack in the direction of the tip is certified at near-tip enrichment that disappears in the direction of this tip [43-45]. As mentioned in [44], the polar coordinate in the direction of a crack tip is not well-explained at the twists. While the areas covering LEFM answers are defined for low strains, they are not used for enormous strains. This situation makes it difficult to find the enrichment section close to the tip. Therefore, an improved method had to developed [46].

7 Result and Discussion

In this paper, a new direct coupling method is used to analyze an infinite plate with a central crack using two different approaches. The first technique, i.e. "the separate method", uses separate elements along a crack, while the second one, i.e. "the continuous method", uses continuous elements. In all the figures, the obtained results concern the plane strain condition, dmax is the domain of the influence and nnx is the number of particles in the enriched EFG method. The variation of the energy error norm is shown in Fig. 4-a for these two methods. As seen, the energy error of these two methods increases by increasing the length of the crack. In Fig. 4-b, it can be seen that nnx=16 leads to the best results. Figure 5 shows the trend of maximum displacement error by changing dmax. As seen in these plots, error in both methods will decrease by increasing dmax maximum. The best dmax is between 2-2.6. Also, we use different weight functions to solve this problem. The best weight function in this case is exponential weight function. In Fig. 5, the results of two different loads and are shown. is the load we named "increased load".

Figure 6 compares the variation of SIF with crack length changing of the exact solution, the coupled method and the enriched method. As depicted, the error of the coupled method from the exact solution is bigger than that of the enriched method but the two graphs (EFG and the coupled method) are very similar to each other.

Fig's. 7 -10 illustrate the results of the two approaches. We have applied 16 and 4 elements in the FEM field and this can be seen in Fig's. 7-10. From these four plots, the following results are obtained: using four elements in the FEM field provides more precise answers than using 16 elements. The result of the continuous method is better than those of the separate method. In Fig. 7-b, "tip nodes" are those nodes near the crack tip and "split node" are located on both sides of the crack trajectory.

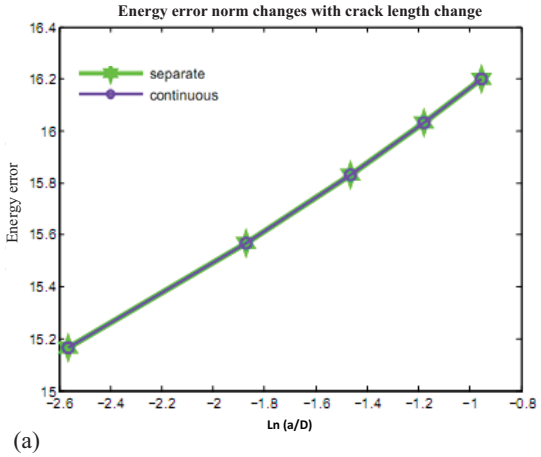

(a)

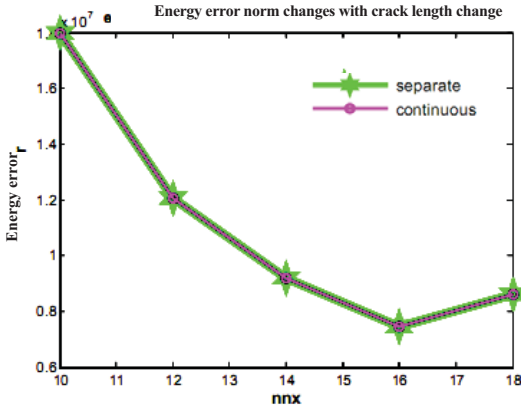

Figure 4. (a) the variation of energy error by changing a/D for the separate and continuous methods, (b) the variation of energy error by changing the number of nodes in the EFG region and using the separate and continuous methods. (Both figures are related to mode I.)

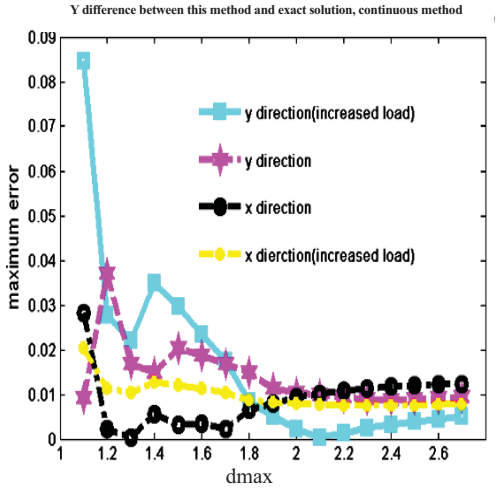

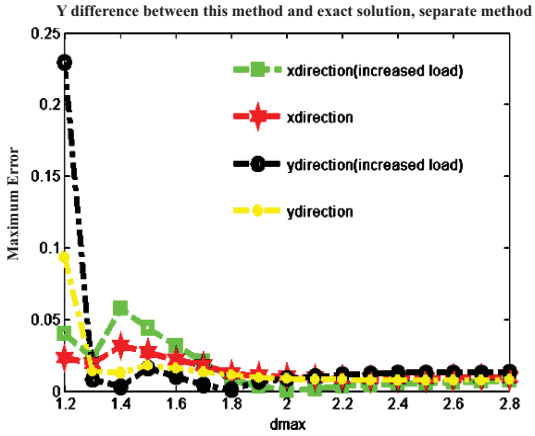

Figure 5. The changing of maximum displacement error with respect to dmax: (a) the continuous method, (b) the separate method.

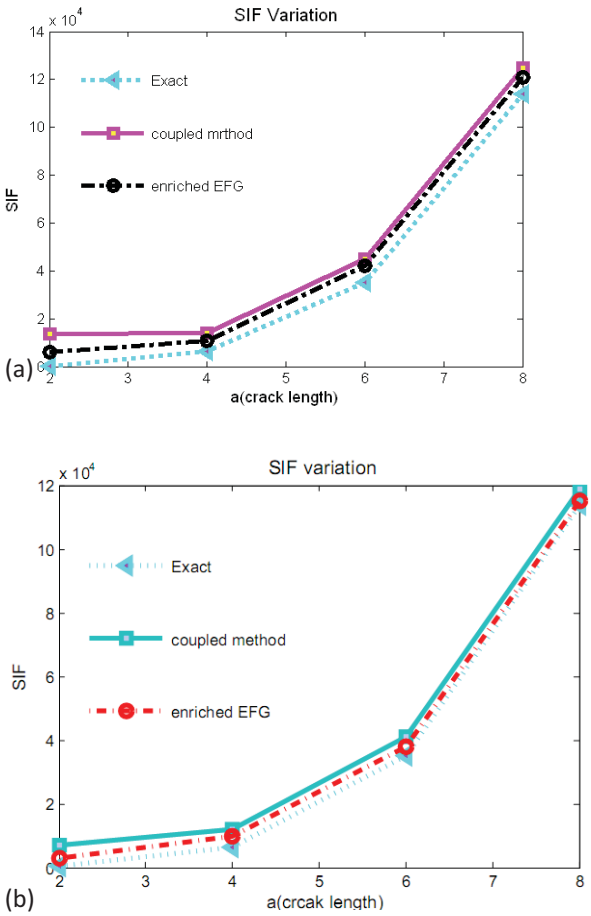

Figure 6. The variation of SIF in the coupled method with crack length change compared with analytical solutions: (a) Using 4 elements and 14 particles, (b) Using 32 elements and 14 particles.

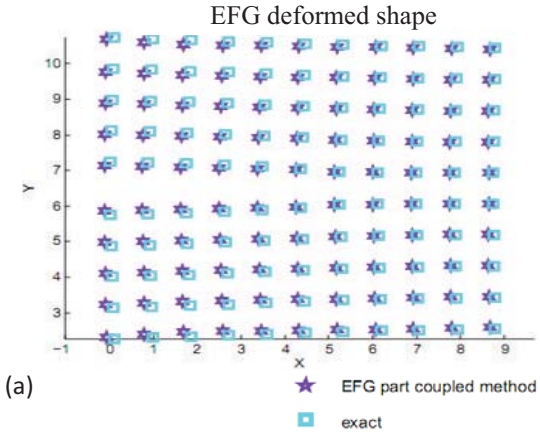

Figure 7. The separate method with 16 elements in the FEM field: (a) displacement of the EFG part of the coupled method compared with exact displacement, (b) fantom nodes, (c) displacement of the FEM part of the coupled method compared with exact displacement, (d) deformed shapes of the two fields, (e) tension distribution of the coupled method, (f) exact tension distribution. Conditions: D =13 nu = 0.3 = E = a =5 nnx =14 dmax =1.7

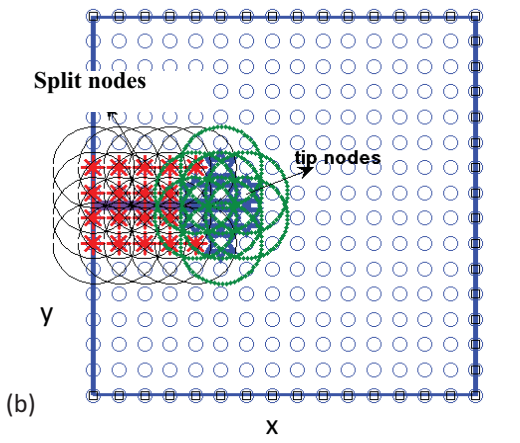

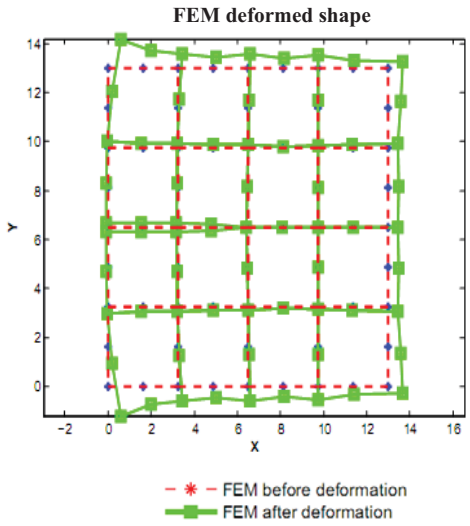

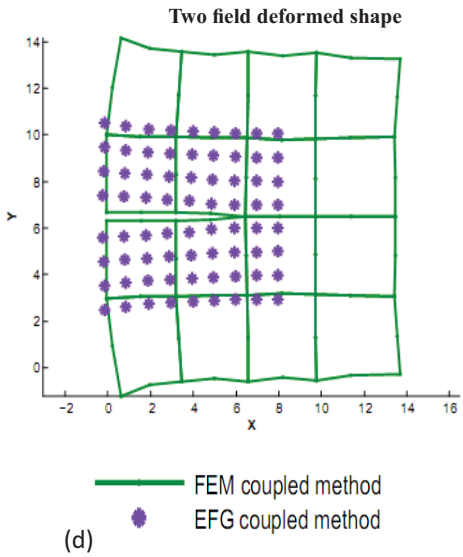

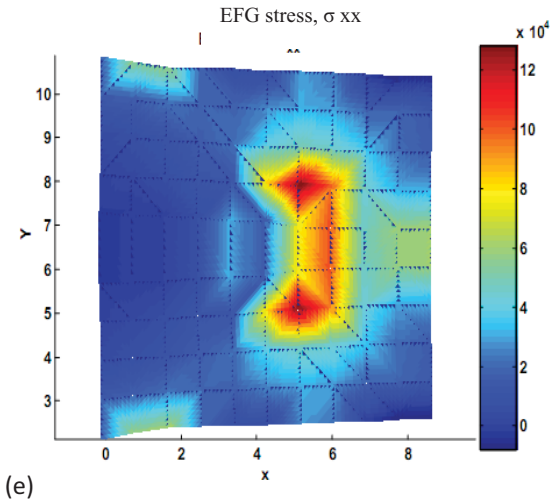

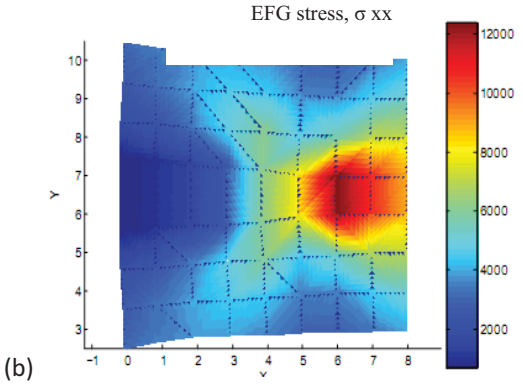

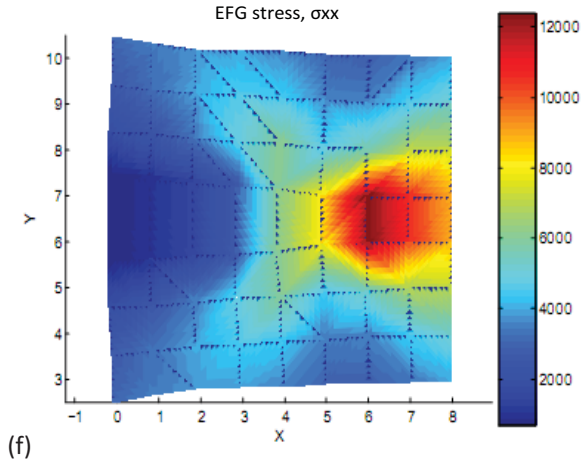

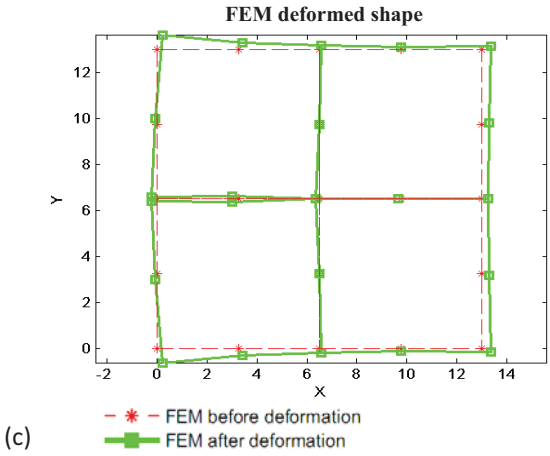

Figure 7. Cont'd.

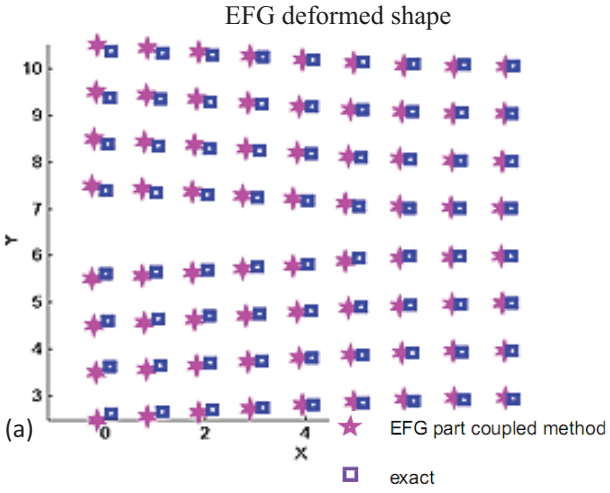

Figure 8. Results of the separate method with 4 elements in the FEM field: (a) displacement of the EFG part of the coupled method compared with exact displacement, (b) tension distribution, (c) Displacement of the FEM part of the coupled method compared dith exact displacement, (d) deformed shapes of the two fields. Condition: D =13; nu = 0.3; = ;E = ;a =5;nnx =14;dmax =1.6

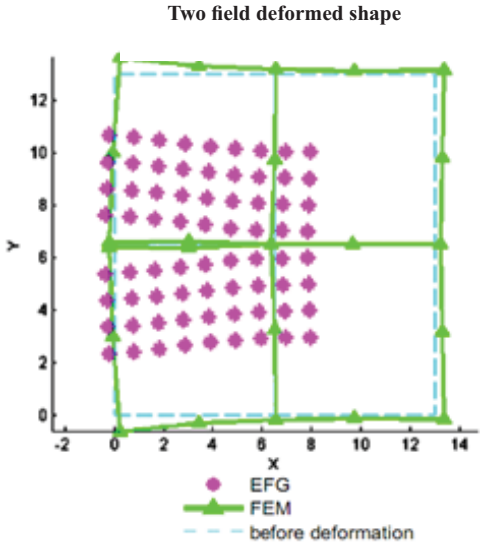

Figure 8. Cont'd.

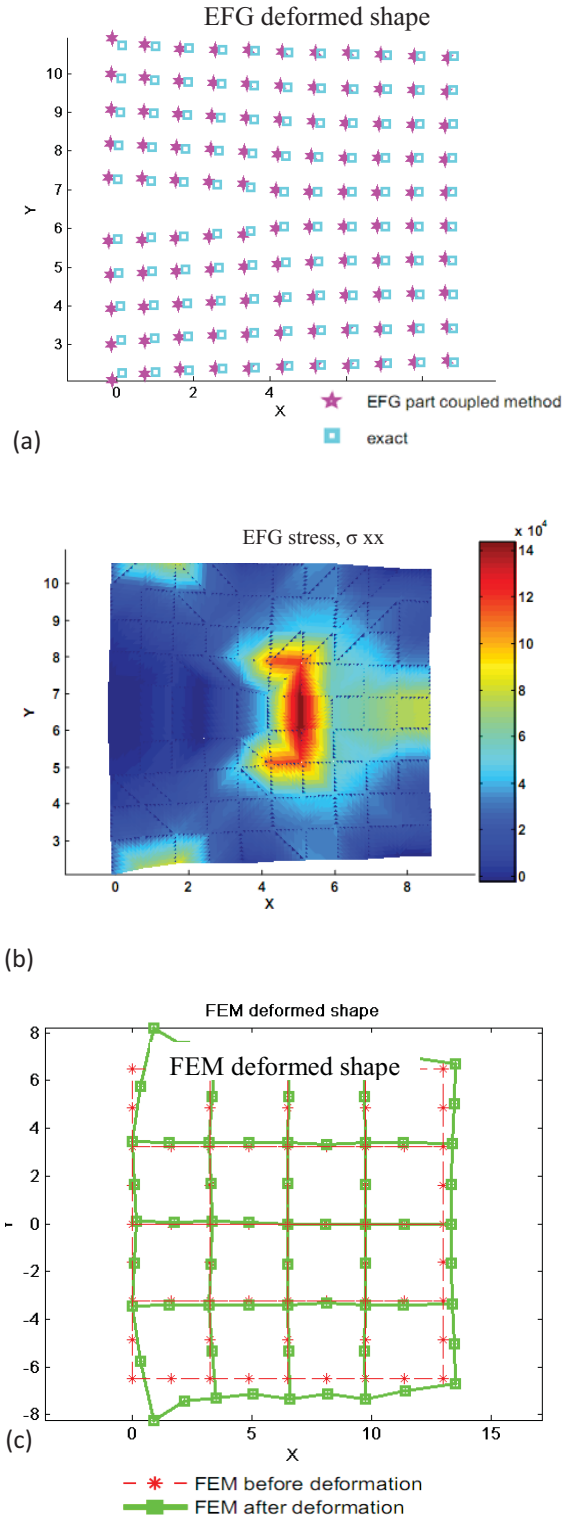

Figure 9. The continuous method with 16 elements in FEM field: (a) displacement of the EFG part of the coupled method compared with exact displacement, (b) tension distribution, (c) displacement of the FEM part of the coupled method compared with exact displacement, (d) deformed shapes of the two fields. Condition: D =13;nu = 0.3; σ = 1 0^4;E = 3 0×1 0^6 ;a =5 nnx =14 ;dmax =1.6;

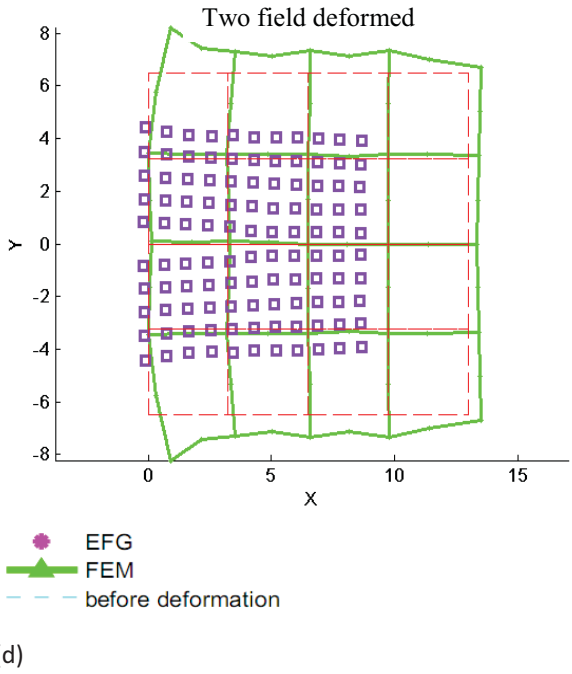

Figure 9. Cont'd.

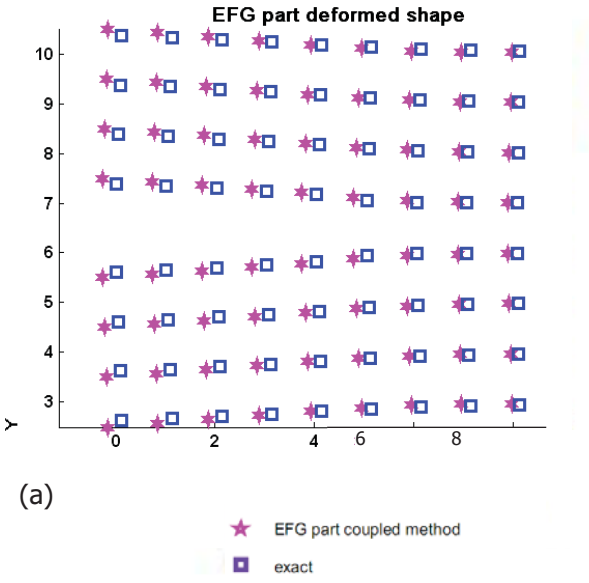

Figure 10. The continuous method with 4 elements in FEM field: (a) displacement of the EFG part of the coupled method compared with exact displacement, (b) tension distribution, (c) displacement of the FEM part of the coupled method compared with exact displacement, (d) deformed shapes of the two fields. Condition: D =13;nu = 0.3; σ = 1 0^4;E = 3 0×1 0^6 ;a =5 nnx =14 ;dmax =1.6;

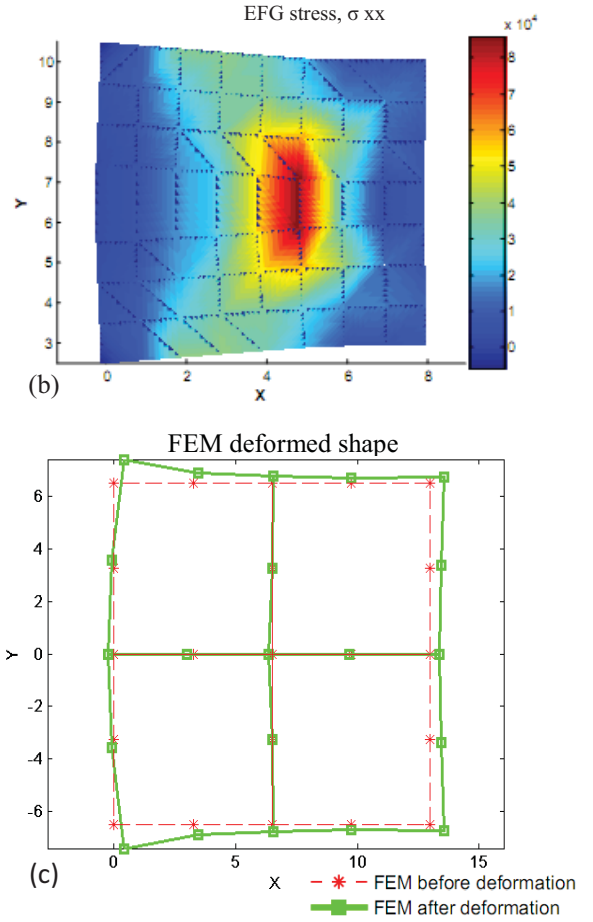

Figure 10. Cont'd.

8 Concluding Remarks

The FEM has fundamental troubles in fracture mechanics problems due to its inadequacy in re-meshing. Meshfree methods are efficient for crack problems but they are usually very time-consuming.

Studies of crack problems reveal that a crack area commonly occupies just a little section in the whole problem field. Meshless methods have a lot of advantages to model a crack in comparison with the FEM, but the FEM has some benefits to model the other regions far from the crack. It is acceptable and advantageous to combine meshless methods with the FEM in order to use their profits and avoid their defects.

A new combined meshless/FEM method proposed by Hsun and Ping [19] has been utilized in this work to study crack problems. The meshless method was applied just in a sub-domain embracing the crack and the remaining section was modeled by the FEM.

Numerical samples were investigated to check the reliability of this combined method for crack problems and excellent answers were obtained. The combined method maintains the benefits of the FEM and EFG including: (1) low computational expense, (2) excellent accuracy. Thus, it can be concluded that the present combined method is an advantageous and effective technique for the study of crack problems.

9 References

1. Zienkiewicz, O.C., and Taylor, R.L., "The Finite Element Method", 4th ed, McGraw-Hill, (1989).

2. Cook, R.D., Malkus D.S., and Plesha, M.E., *"Concepts and Applications of Finite Element Analysis"*, 3rd Ed, John Wiley and Sons, (1989).

3. Phu N.V., Rabzuck T., Bordas S., and Duflot M., "Meshless Methods: A Review and Computer Implementation Aspects", Mathematics and Computers in Simulation, **79**(3), pp. 763-813 (2008).

4. Monaghan J.J., "An introduction to SPH computer Physics Communications", **48**(1), PP 89-96(1982).

5. Gingold R.A., Moraghan J.J., "Smoothed particle hydrodynamics: theory and applications to non-spherical stars", *Mon. Not. Astronom.Soc*. **181**, PP 375–389(1977).

6. Lucy L.B.," A numerical approach to testing of the fission hypothesis Astron "J.**8**, PP 1013-1024(1977).

7. Nayroles B., Touzot G., and Villon P., "Generaliz-

ing the Finite Element Method: Diffuse Approximation and Diffuse Elements", Computational Mechanics, **10**(5), PP 307-318(1992).

8. Belytschko, T., Lu, Y.Y and Gu, L., "Element Free Galerkin Method", *International Journal for Numerical Methods in Engineering*,**37**(2), PP 229-256. (1994).

9. Krysl, P. and Belytschko, T." Element-free Galerkin method: Convergence of the continuous and discontinuous shape functions", *Comput. Methods Appl. Mech. Eng.,* **48**(3-4)PP 257-277, (1997).

10. Belytchko, T., Felming M., Organ D., Krongauz Y., Liu WK.," Smoothing and accelerated computations in the element free Galerkinmethod "*J. Comput. Appl. Math.* **74**, PP 111–126(1996).

11. Chen.J.S., Pan C., Wu C.T., Liu W.K., "Reproducing kernel particle methods for large deformation analysis of non-linear structures", *Comput. Methods Appl. Mech. Engrg.***139** (1–4), PP195–227 (1996).

12. Liu, G.R., Gu, Y.T., "Meshless local Petrov–Galerkin (MLPG) method in combination with finite element and boundary element approach", *Comput. Mech.***26** (6), PP536–546(2000).

13. Atluri S.N., Zhu T., "A new meshless local Petrov-Galerkin (MLPG) approach in computational mechanics", *Computational Mechanics***22**, PP 117–127. (1998).

14. Hegen D.," Element free Galerkin methods in combination with finite element approach", *Comput .Methods Appl .Mech. Engrg*.135, PP143-166(1996).

15. Belytschko T., Organ D., Kronguaz Y., A coupled finite element–element free Galerkin method", *ComputMec*17(3)(1995).

16. Rao.B.N.,S.Rahman "A coupled meshless-finite element method for fracture analysis of crack", *International Journal of pressure Vessels and Piping***78**, PP 647-657(2001).

17. Gu.Y.T., Zhang L.C., "Coupling of the meshfree and finite element methods for determination of the crack tip field", *Engineering Fracture Mechanics*, **75**, PP 986-1004(2008).

18. Xiao Q.Z., Dhanasekar M., "Coupling of FE and FEG using collocation approach", *Advanced in Engineering Software***, 33**, PP 507-515(2002).

19. Chien-Hsun L., and Chan-Ping P.," Conjunction of Displacement Fields of the Element Free Galerkin Method and Finite Element Method".*Tamkang Journal of Science and Engineering,***10**(1), PP 41-50(2007).

20. Krongauz Y., Belytschko T., "EFG approximation with discontinuous derivatives", *Int. J. Numer. Methods Eng.***41,** PP 1215–1233(1998).

21. Organ D., Fleming M., Terry T., Belytschko T., "Continuous meshless approximations for nonconvex bodies by diffraction and transparency", *Comput. Mech*. **18** , PP 225–235(1996).

22. Fleming M., Chu Y.A., Moran B., BelytschkoT., "Enriched element-free Galerkin methods for crack tip fields", *Int. J. Numer. Methods Eng***. 40**, PP 1483–1504(1997).

23. Ventura G., Xu J.X., Belytschko T., "A vector level set method and new discontinuity approximations for crack growth by EFG", *Int. J. Numer. Methods Eng***. 54**, PP 923–944(2002).

24. Carpinteri A., "Post-peak and post-bifurcation analysis of cohesive crack propagation", *Eng. Fract. Mech*. **32**, PP 265–278(1989).

25. Carpinteri A., "A scale-invariant cohesive crack model for quasi-brittle materials", *Eng. Fract. Mech*. **69**, PP 207–217(2002).

26. Belytschko,T. Lu,Y.Y and Gu,L. "Element Free Galerkin Method", *International Journal for Numerical Methods in Engineering*,**37**(2), PP 229-256(1994).

27. Nayroles B., Touzot G., and Villon P., "Generalizing the Finite Element Method: Diffuse Approximation and Diffuse Elements", *Computational Mechanics*, 10(5), PP 307-318(1992).

28. Lancaster P., Salkauskas K., "Surfaces generated by moving least squares methods " *,Math. Comput.***37**, PP 141-158(1981)

29. Nakai D., Kawahara M.," A Numerical Analysis Equation Using Element-Free Galerkin Method", *KAWAHARALAB,*VOL,3Nov,PP14(2002).

30. Fleming M., Chu Y.A., Moran B., and Belytschko T., "Enriched element-free Galerkin methods for crack tip fields", *International Journal for Numerical Methods in Engineering,* **40**, PP1483–1504 (1997).

31. Guang-ming Z., shun-cheng S., "Applied Mathematics and Mechanics element and meshless methods", *Int. J. Numer.Methods.Engrg*.**48**, PP 1615–1636(2000).

32. Huerta A., Ferna´ndez-Me´ndez S., "Enrichment

and coupling of the finiteelement and meshless methods, Int. J. Numer. Methods Eng, 48(11), PP 1615–1636(2000).

33. Portela A., Aliabadi M.H., "The dual boundary element method: effective implementation for crack problems",.*Int J Numer Meth Engng* ,**33**, PP 1269–87(1992).

34. Mccarron A.P., "A synergistic approach to modeling crack propagation in nanoreiforced polymer composites",*MSC thesis, University of Massachusetts Amherst,* May (2008).

35. Huber, O., Nickel J., Kuhn G., "On the decomposition of the J-integral for 3D crack problems", *Int J Fract*, **64**, PP 339–48(1993).

36. Belytschko, T., Black T., "Elastic crack growth in finite elements with minimal remeshing". *Int J Numer Meth Engng*,**45**(5), PP601–20(1999) .

37. Belytschko, T., Tabbara M., "Dynamic fracture using element-free Galerkin methods". *Int J Numer Meth Engng*; **39**(6),PP923–38(1996).

38. Lu Y., Belytschko T., Tabbara M., "Element-free Galerkin method for wave-propagation and dynamic fracture". *Comput Meth ApplMechEngng*,**126**(1–2),PP131–53(1995).

39. Belytschko T., Lu Y., "Element-free Galerkin methods for static and dynamic fracture", *Int J Solids Struct*, **32**, PP 2547–70(1995).

40. Belytschko T., Lu Y., Gu L., "Crack propagation by element-free Galerkin methods",*EngngFractMech*, **51**(2), PP 295–315(1995).

41. Krysl P., Belytschko T., "The element free Galerkin method for dynamic propagation of arbitrary 3-D cracks".*Int J Numer Meth Engng*, 44(6), PP 767–800(1999).

42. Ventura G., Xu J., Belytschko T., "A vector level set method and new discontinuity approximations for crack growth by EFG", *Int J Nu0mer Meth Engng*,**54**(6), PP 923–44(2002).

43. Rabczuk T., Zi G., "A meshfreemethod based on the local partition of unity for cohesive cracks", *ComputMech***39**(6), PP 743–60(2007).

44. Rabczuk T., Bordas S., Zi G., "A three-dimensional meshfree method for continuous multiple-crack initiation, propagation and junction in statics and dynamics", *ComputMech*, in online, doi:10.1007/s00466-006-0122-1.(2006).

45. Rabczuk T., Areias P., "A meshfree thin shell for arbitrary evolving cracks based on an external enrichment".*Comput Model EngngSci*,**16**(2):115–130 (2006).

46. Brighenti R.," Application of the element-free Galerkinmeshless method to 3-D fracture mechanics problems", *Engineering Fracture Mechanics,* **72**, PP 2808–2820(2005)